Published OnlineFirst December 15, 2010; DOI: 10.1158/0008-5472.CAN-10-3757

Fes Tyrosine Kinase Expression in the Tumor Niche Correlates with Enhanced Tumor Growth, Angiogenesis, Circulating Tumor Cells, Metastasis, and Infiltrating Macrophages

Shengnan Zhang[1], Violeta Chitu[2], E. Richard Stanley[2], Bruce E. Elliott[1], and Peter A. Greer[1]

Abstract

Fes is a protein tyrosine kinase with cell autonomous oncogenic activities that are well established in cell culture and animal models, but its involvement in human cancer has been unclear. Abundant expression of Fes in vascular endothelial cells and myeloid cell lineages prompted us to explore roles for Fes in the tumor microenvironment. In an orthotopic mouse model of breast cancer, we found that loss of Fes in the host correlated with reductions in engrafted tumor growth rates, metastasis, and circulating tumor cells. The tumor microenvironment in Fes-deficient mice also showed reduced vascularity and fewer macrophages. In co-culture with tumor cells, Fes-deficient macrophages also poorly promoted tumor cell invasive behavior. Taken together, our observations argue that Fes inhibition might provide therapeutic benefits in breast cancer, in part by attenuating tumor-associated angiogenesis and the metastasis-promoting functions of tumor-associated macrophages. *Cancer Res; 71(4); 1465–73. ©2010 AACR.*

Introduction

The *fes* proto-oncogene (also known as *fps*), encodes a Src homology 2 (SH2) domain-containing cytoplasmic protein-tyrosine kinase (PTK) which has been implicated in signaling downstream of receptors for cytokines, growth factors, immunoglobulin, collagen, and endotoxin (reviewed in refs. 1 and 2). Fes expression is restricted to myeloid, endothelial, and subsets of epithelial and neuronal cells (1, 3, 4). Fes was originally identified as a dominant-acting oncoprotein encoded by transforming retroviruses isolated from avian (*fps*; ref. 5) or feline (*fes*; ref. 6) tumors. When expressed in transgenic mice, viral *fps* induced tumors in lymphoid and mesenchymal tissues (7). These observations suggested that activating mutations in the human *fes* proto-oncogene might contribute to cancer. Missense mutations were subsequently identified in human colorectal cancers (8), leading to the speculation that activated Fes kinase contributed to these cancers. However, subsequent biochemical and structural modeling analysis revealed that these mutations attenuated rather than activated Fes kinase (9). This revelation raised the novel possibility that Fes might also function as a tumor suppressor. Genetic evidence to support this hypothesis came from studies of transgenic mice expressing polyoma virus middle T (PymT) antigen in the mammary glands. Tumors developed earlier in mice targeted at the *fes* locus with either null or kinase-inactivating missense mutations (9). The *fes* promoter was also found to be silenced by methylation in colorectal cancer cell lines, and this correlated with downregulation of Fes expression (10). These apparently contradicting observations argued that Fes may play both oncogenic and tumor suppressor roles. Furthermore, considering the different cell types which express Fes, the cumulative effect on tumorigenesis may depend on both tumor autonomous cell roles and roles in cells of the tumor niche. For example, tissue-specific expression of an activated *fes* allele in transgenic mice led to hypervascularity and multifocal hemangiomas correlating with expression in vascular endothelial cells (11), and this same activated *fes* allele was able to partially rescue the vasculogenesis defect in vascular endothelial growth factor (VEGF) receptor knockout embryos (12). In other studies using *fes* knockout mice, we observed hypersensitivity to endotoxin, which correlated with abundant Fes expression in macrophages where it regulates TLR4 endocytosis, NFκB signaling, and TNFα expression (13, 14). These phenotypes in transgenic and knockout mice suggested possible roles for Fes in both vascular endothelial and myeloid cells, which might influence tumor progression. Tumor cell autonomous roles for Fes in breast cancer initiation were also suggested by a recent study showing Fes is highly expressed

Authors' Affiliations: [1]Division of Cancer Biology and Genetics, Department of Pathology and Molecular Medicine, Queen's Cancer Research Institute, Queen's University, Kingston, Ontario K7L3N6, Canada; and [2]Department of Developmental Biology and Molecular Biology, Albert Einstein College of Medicine, Bronx, New York

Note: Supplementary data for this article are available at Cancer Research Online (http://cancerres.aacrjournals.org/).

Corresponding Author: Peter A. Greer, Division of Cancer Biology and Genetics, Department of Pathology and Molecular Medicine, Queen's University, Queen's Cancer Research Institute, Kingston, Ont. K7L3N6, Canada. E-mail: greerp@queensu.ca.

doi: 10.1158/0008-5472.CAN-10-3757

©2010 American Association for Cancer Research.

Downloaded from cancerres.aacrjournals.org on May 16, 2021. © 2011 American Association for Cancer Research.

Published OnlineFirst December 15, 2010; DOI: 10.1158/0008-5472.CAN-10-3757

and activated in mouse mammary epithelial cells during lactation, where it is associated with E-cadherin based adherens junctions (4). However, to our knowledge, Fes expression in breast tumors or tumor cell lines has not been reported.

To elucidate the involvement of Fes in breast cancer, we have employed a tumor cell orthotopic mouse mammary gland engraftment model designed to separately examine tumor cell autonomous and niche roles of Fes. Manipulation of Fes expression in the engrafted breast carcinoma cells had no effect on growth at the orthotopic injection site or metastasis. However, when Fes expression was eliminated in the niche, significant reductions in tumor growth rates and metastasis were observed. These defects correlated with reductions in tumor-associated vascularity, macrophages, and circulating tumor cells. Bone marrow–derived *fes-null* macrophages were less proficient at promoting the *in vitro* invasive properties of cocultured tumor cells, or of being induced to invade by tumor cells. These observations are consistent with tumor progression roles of Fes acting at the level of the vascular endothelial cells and macrophages. This study provides novel genetic evidence that the Fes protein-tyrosine kinase represents a potential therapeutic target in breast cancer, where Fes inhibition in macrophages and vascular endothelial cells would attenuate their tumor promoting roles.

Materials and Methods

Cell culture

The highly metastatic AC2M2 mouse mammary carcinoma cell line (15) was routinely cultured in Dulbecco's Modified Eagle Medium (Invitrogen) supplemented with 10% fetal bovine serum (FBS, Sigma), 2 mM L-glutamine and antibiotics/antimycotics (Invitrogen), and maintained at 37°C with 5% CO_2 in a humidified incubator. These cells were transduced with lentivirus expressing green fluorescence protein (GFP). For some experiments, these GFP-expressing AC2M2 cells were transduced with pMSCVpuro (Clontech) retroviruses encoding C-terminally Myc-epitope tagged wild type, kinase-dead (K588R; ref. 16), or kinase-activated (*N*-terminally myristoylated) Fes (11).

Mice

The previously established *fes-null* ($fes^{-/-}$) strain (13) was crossed with nude mice (NCr-$Foxn1^{nu/nu}$; Taconic) to produce hybrid wild-type ($fes^{+/+}$; *nu/nu*) and *fes-null* nude ($fes^{-/-}$; *nu/nu*) mice. Mice were housed in the Animal Care Facility and procedures were carried out according to the guidelines of the Canadian Council on Animal Care, with the approval of the institutional animal care committee.

Orthotopic mammary gland engraftment model

After being anesthetized with 250 mg/kg avertin, age-matched wild-type and *fes-null* female nude mice were injected with 7,500 GFP-expressing AC2M2 cells into the fourth mammary gland (15). Tumor growth at the orthotopic site was measured by ultrasound imaging (VisualSonics Vevo 770) 12, 14, 16, 19, and 22 days after engraftment. On day 23, the tumors were removed and mice were kept alive to assess metastasis. On day 35, mice were euthanized, lungs were dissected, and GFP-expressing metastatic nodules were biophotonically imaged using a Pan-A-See-Ya Panorama imaging system. Images were captured using a Hamamatsu B/W ORCA-ER digital camera with excitation filter at 470 nm/20 nm and an emission filter at 525 nm/20 nm.

In vivo macrophage imaging

Mice were engrafted with AC2M2 cells as described earlier. On day 13, these tumor-bearing mice were injected with 200 μL of 20 mg/mL tetramethylrhodamine conjugated dextran beads (Invitrogen). After 2 hours, mice were perfused with 1% paraformaldehyde in PBS and mammary glands were dissected and imaged by Leica TCS SP2 confocal microscopy.

Flow cytometry measurement of macrophages and endothelial cells

Tumor-bearing mammary glands were harvested from wild-type and *fes-null* nude mice 7 days after engraftment as described earlier, and digested in tissue digestion buffer containing 0.1 mg/mL collagenase (Sigma), 0.072 mM $CaCl_2$ and 20% FBS at 37°C for 3 hours. Single-cell suspensions were obtained by filtering twice through 70 μm cell strainers (BD Bioscience). Samples were centrifuged at 700 rpm for 5 minutes, and resuspended in 2 mL ice-cold PAB [phosphate-buffered saline with 1% (w/v) bovine serum albumin]. Aliquots were incubated with 0.1 μg/mL phycoerythrin (PE)-conjugated rat antimouse F4/80 antibody (Caltag) for macrophages, PE-conjugated rat IgG2a (Molecular Probes) for isotype control, or propidium iodide (Invitrogen) for cell viability. Samples were then washed with ice-cold PAB, fixed for 15 minutes with 2% formaldehyde (Sigma) at 37°C, resuspended in 500 μL PAB, and analyzed by flow cytometry. Peritoneal macrophages (obtained as described previously; ref. 14) were used as positive controls.

Immunoblotting

Lysates from mammary glands, tumors, or cell cultures were prepared in RIPA lysis buffer and assessed by immunoblotting as described in detail previously (4). Protein levels were determined by densitometry using Image Pro software. Antibodies used in immunoblotting included anti-Fes, which is a rabbit polyclonal serum that cross-reacts with Fes and Fer (α-FpsQE; ref. 3), anti-Myc ascites (1–9E10.2 mouse hybridoma from American Type Culture Collection), anti-RasGap rabbit polyclonal (17), anti-tubulin mouse monoclonal (Sigma), or anti-PECAM-1, which is rabbit polyclonal serum raised against a GST-fusion protein containing the complete cytoplasmic domain of mouse PECAM-1 (18).

Immunofluorescence analysis of tumors and stroma

Tumors and associated mammary glands were removed from age-matched wild-type and *fes-null* mice 7 days after engraftment, fixed in 4% paraformaldehyde, and paraffin embedded. Tissue sections (5 μm) were deparaffinized with toluene and rehydrated through an ethanol gradient. Antigen was retrieved by heating sections in 10 mM sodium citrate

Downloaded from cancerres.aacrjournals.org on May 16, 2021. © 2011 American Association for Cancer Research.

Published OnlineFirst December 15, 2010; DOI: 10.1158/0008-5472.CAN-10-3757

(pH 6.0) at 95°C in a steam cooker for 20 minutes. After cooling at room temperature for 20 minutes, sections were rinsed 3 times with PBS, and incubated in 0.2% Triton/PBS for 10 minutes, followed by 3 PBS rinses. Sections were then blocked with 3% BSA for 20 minutes. Following 3 washes in PBS, sections were incubated overnight with PECAM-1 rabbit polyclonal antibody (1:50 dilution in blocking buffer) at 4°C. Sections were washed 3 times in PBS before addition of Alexa Fluor 546 goat antirabbit IgG (1:200 dilution in blocking buffer, Invitrogen) for 1 hour at room temperature. After thorough washing with PBS, sections were mounted with Mowiol (Calbiochem) and imaged using Olympus BX51 fluorescence microscopy with excitation filter at 545 nm and emission filter at 576 nm. Quantification of vasculature in tumor stoma was performed using Image Pro software.

Tail vein injection lung metastasis model

Five $\times$ 10^5 GFP-expressing AC2M2 cells were injected into the tail veins of wild-type or *fes-null nu/nu* mice and 22 days later lungs were dissected and biophotonically imaged as described earlier. Numbers and sizes of metastatic lesions were determined using Image Pro software.

Detection of circulating tumor cells

Twenty-two days after engraftment with GFP-expressing AC2M2 cells, peripheral blood was collected by cardiac punctures performed under deep anesthesia with isofluorane. Five hundred microliters of blood samples were subjected to hypotonic shock with 5 mL distilled water, followed by isotonic restoration with 1.5 mL 0.6M KCl. Samples were then washed with 50 mL PBS to remove red blood cell debris, resuspended in 500 μL PAB, and analyzed by flow cytometry.

Collagen invasion assay

Primary bone marrow–derived macrophages were obtained as previously described (19). MTLn3-GFP rat breast cancer cells were cocultured for 18 hours with bone marrow–derived macrophages (BMM) from wild-type or *fes-null* mice in the presence of colony stimulating factor (CSF)-1 and 10% FBS. Cocultures were then overlaid with collagen I gels and invasion into the collagen gel after 24 hours was quantified as previously described (20).

Statistics

All statistical analysis was done by using GraphPad Prism 5 software. All error bars represent standard error of the mean (SEM). *P* values were calculated by Student's *t*-test and 2-way analysis of variance (ANOVA) analysis. Data sets with $P \leq 0.05$ were considered statistically significant.

Results

Fes plays a tumor-promoting role in the niche

Preliminary experiments were performed to explore potential tumor cell autonomous roles for Fes in mammary tumorigenesis. GFP-expressing AC2M2 mouse breast carcinoma cells were transduced with retroviruses encoding wild-type, kinase-dead, or activated Fes (Supplementary Fig. S1A). These cells were engrafted into the mammary glands of *nu/nu* mice and tumor growth was monitored by ultrasound measurement for 22 days. Primary tumors were then removed to promote metastatic growth and lung metastasis was examined 13 days later. No significant differences in tumor growth rates at the orthotopic injection site were observed (Supplementary Fig. S1B) and there were no significant differences in the frequency of metastasis to the lungs (data not shown). Thus, Fes did not appear to play a tumor cell autonomous role in this AC2M2 tumor engraftment model.

We next asked whether Fes expression in the niche cells, rather than in tumor cells, might influence tumor growth and metastasis. To facilitate these experiments, we crossed *nu/nu* mice with *fes* knockout mice (13) and established colonies of wild-type and *fes-null nu/nu* mice. GFP-expressing AC2M2 cells were orthotopically engrafted into the mammary glands of wild-type and *fes-null nu/nu* mice and tumor growth and metastasis was monitored as described earlier. Tumor growth at the orthotopic site was significantly slower in *fes-null* mice ($P < 0.0001$) relative to wild-type mice (Fig. 1) and the frequency of lung metastasis was also significantly reduced in *fes-null* mice, with 70% of wild-type mice versus 50% of *fes-null* mice developing metastasis (Supplementary Fig. S2). Also, among mice displaying lung metastasis wild-type mice displayed significantly more metastatic nodules ($P = 0.0055$; Fig. 2A). Although there was a trend toward smaller sized metastatic lung nodules in the *fes-null* mice, this difference did not achieve statistical significance ($P = 0.1215$; Fig. 2B).

Reduced vascularity in the *fes-null* tumor niche

The reduction in tumor engraftment growth rate and metastasis frequency in *fes-null* mice suggested Fes might be playing a tumor promoting role, which is intrinsic to cells making up the tumor niche. Angiogenesis promotes tumor growth and metastasis, and Fes is expressed in vascular

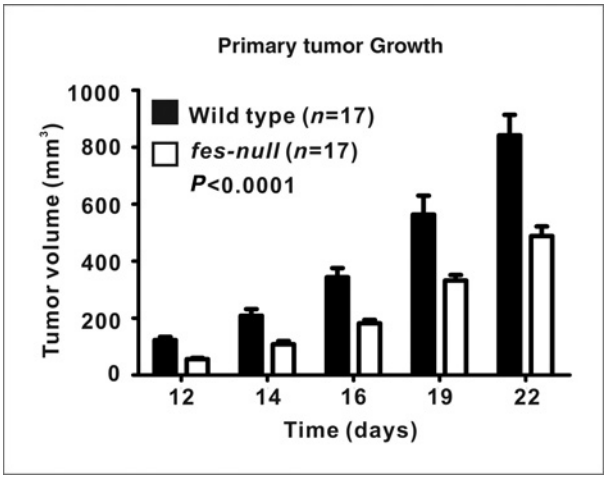

Figure 1. Orthotopic tumor growth rates were reduced in fes-null mice. AC2M2 cells were engrafted into mammary glands of wild-type and *fes-null nu/nu* mice and tumorigenesis was assessed by ultrasound imaging over a period of 22 days. Tumor growth rates were significantly slower in *fes-null* relative to wild-type mice ($P = 0.0001$; $n = 17$ for both groups).

Downloaded from cancerres.aacrjournals.org on May 16, 2021. © 2011 American Association for Cancer Research.

Published OnlineFirst December 15, 2010; DOI: 10.1158/0008-5472.CAN-10-3757

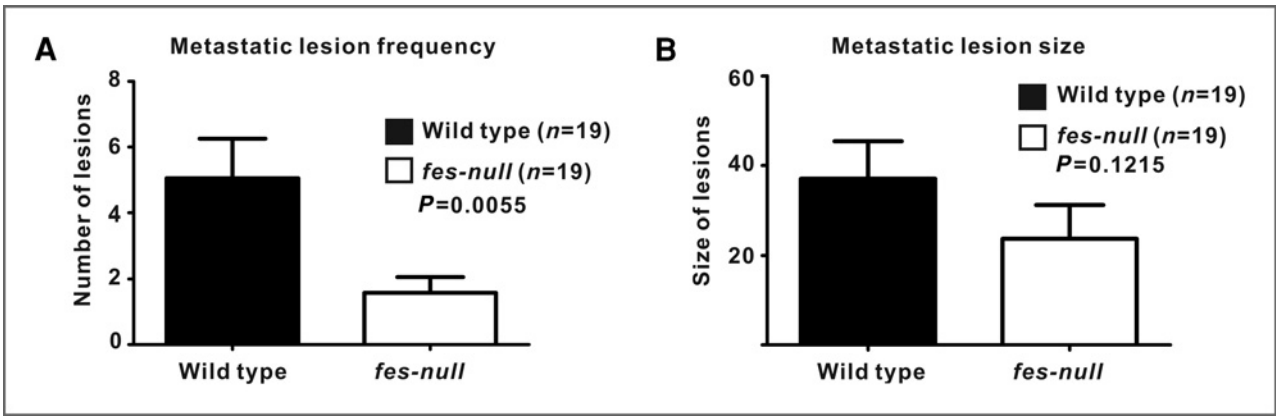

Figure 2. Reduced metastasis in fes-null mice. AC2M2 cells were engrafted into wild-type and *fes-null* mice and allowed to grow for 22 days. Tumors were then removed to promote tumor growth at metastatic sites and lungs were removed for biophotonic imaging of metastatic lesions 13 days later. A, significantly more metastatic lesions per lung were observed in wild-type relative to *fes-null* mice lungs ($P = 0.0055$; $n = 19$ for each group). B, the size of metastatic lesions (as assessed by pixel numbers per lesion) in *fes-null* mice appeared somewhat smaller than in wild-type mice, but this difference did not reach statistical significance ($P = 0.1215$).

endothelial cells and has been implicated in angiogenesis (11, 12, 21–23). We therefore examined the vascularity in wild-type and *fes-null* tumors and associated tissues. PECAM-1 immunofluorescence staining revealed reduced numbers of blood vessels in *fes-null* stroma (Supplementary Fig. 3). Quantification of these data showed a significant reduction in vessel density in *fes-null* tumor stroma ($P = 0.0251$; Fig. 3A). When the percentages of vessels of different sizes were compared, we found that the reduced vascularity was not associated with any particular size of vessels (Fig. 3B).

To further quantify the vascular content of tumors and associated stroma, we next performed quantitative immunoblotting analysis using PECAM-1 antibody. Tumors were allowed to grow for 7 days after AC2M2 cell injection. Lysates were then prepared from dissected tumors (stroma-free), the tumor-associated stroma (tumor-free), as well as from uninvolved mammary glands of tumor-bearing mice or mammary glands of non–tumor-bearing mice. PECAM-1 immunoreactivity was significantly reduced in tumors ($P = 0.0124$; Supplementary Fig. S4A and Fig. 4) and tumor-associated stroma ($P = 0.0284$; Supplementary Fig. S4B and Fig. 4) from *fes-null* mice relative to wild-type mice. There was also a trend toward lower PECAM-1 levels in *fes-null* uninvolved mammary glands from tumor-bearing mice ($P = 0.0580$; Supplementary Fig. S4C and Fig. 4) and mammary glands from non–tumor-bearing control mice ($P = 0.1233$; Supplementary Fig. S4D and Fig. 4), but these differences were not statistically significant.

Reduced involvement of tumor-associated macrophages in *fes-null* mice

Another Fes-expressing cell type that has been implicated in regulating tumorigenesis is the macrophage. In particular, alternatively activated M2-like macrophages are implicated in promoting tumor-associated angiogenesis and metastasis (24–26). We therefore examined the involvement

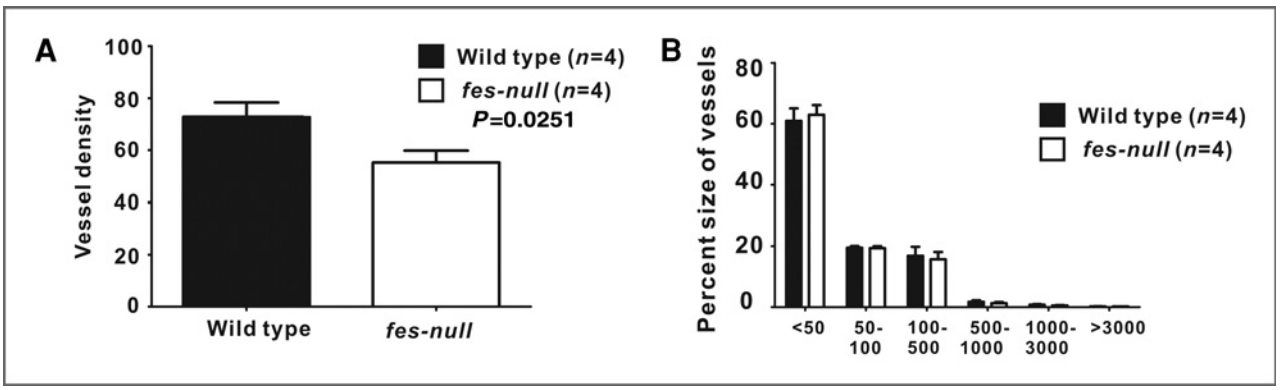

Figure 3. Reduced vascularity in fes-null tumor stroma. AC2M2 cells were engrafted into wild-type and *fes-null* mice. On day 7 postinjection, tumor-bearing mammary glands were dissected, fixed, and paraffin embedded. Five micrometers of tissue sections were deparaffinized and stained with PECAM-1 antibody. Composite images of the stromal tissues surrounding each tumor were assembled and fluorescent pixels in this tumor boundary area were quantified using Image Pro software. The density (A) and size distribution of the blood vessels (B) were determined. Significantly fewer vessels per mm^2 were present in *fes-null* tumor stroma ($P = 0.0251$), but there was no difference in the size distribution of these vessels (<50 pixels, $P = 0.3562$; 50–100 pixels, $P = 0.4460$; 100–500 pixels, $P = 0.1226$; 500–1000 pixels, $P = 0.2371$; 1000–3000 pixels, $P = 0.2222$; >3000 pixels, $P = 0.0790$; $n = 4$ for each group).

Downloaded from cancerres.aacrjournals.org on May 16, 2021. © 2011 American Association for Cancer Research.

Published OnlineFirst December 15, 2010; DOI: 10.1158/0008-5472.CAN-10-3757

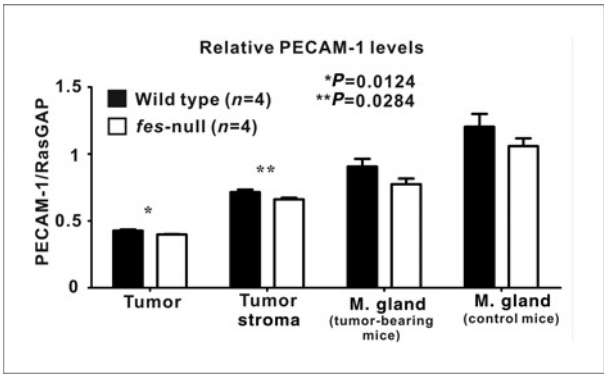

Figure 4. Reduced vascularity in tumors and associated stroma in *fes-null* mice. Wild-type and *fes-null* mice were engrafted with AC2M2 cells and tumors were allowed to grow for 7 days. Tumors were dissected away from associated stroma and separate lysates for each were analyzed by immunoblotting for vascular content using PECAM-1 as a marker for endothelial cells and RasGAP as a protein normalization control (Supplementary Fig. S4). Uninvolved glands from tumor-bearing mice as well as mammary glands from nontumor bearing control mice were also assessed ($n = 4$ for each group). Significantly lower PECAM-1 levels were observed in both tumors ($P = 0.0124$) and stroma ($P = 0.0284$) from *fes-null* mice. Trends toward reduced PECAM-1 levels in *fes-null* mice were also observed in uninvolved mammary glands from tumor-bearing mice ($P = 0.0580$) and mammary glands from nontumor bearing control mice ($P = 0.1233$), but these were not statistically significant.

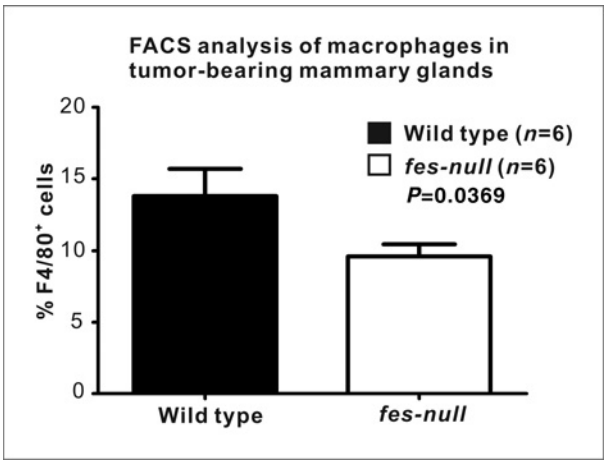

Figure 5. Reduced macrophages in fes-null tumor-bearing mammary glands. Single-cell suspensions were prepared from tumor-bearing mammary glands of wild-type and *fes-null* mice 7 days posttumor cell injection. Cells were stained with PE-conjugated F4/80 antibody to identify macrophages and the relative percentages of stained cells were determined by flow cytometry. There were significantly fewer macrophages in tumor and associated stroma from *fes-null* relative to wild-type mice ($P = 0.0369$; $n = 6$ for both groups).

of macrophages in this engraftment model. Macrophages were initially detected *in vivo* by taking advantage of their propensity to phagocytose dextran beads. Tetramethylrhodamine-conjugated beads were injected i.v. into tumor-bearing mice 13 days after engraftment of GFP-expressing AC2M2 cells. Tumor-bearing mammary glands were removed 2 hours later and imaged by confocal fluorescence microscopy. In wild-type mice, large numbers of dextran-labeled macrophages were clearly observed at the tumor front and within the tumor (Supplementary Fig. S5). In contrast, few macrophages were seen in *fes-null* tumors and associated stroma.

Because Fes-deficiency may have compromised macrophage phagocytosis of dextran beads (14), we also used surface antigen labeling and flow cytometry to quantify macrophages in tumors and surrounding stromal tissues. Single-cell suspensions were prepared from intact tumor-bearing mammary glands removed 7 days after tumor cell injection and the surface antigen F4/80 was used to quantify macrophages. There was a significant reduction in the F4/80$^+$ tumor-associated macrophage content in *fes-null* tumor-bearing mammary glands ($P = 0.0369$; Fig. 5).

Fes-null macrophages are deficient in promoting tumor cell migration and invasion

Tumor-associated macrophages have been shown to correlate with increased neovascularization and poor prognosis in human breast cancer (27). Alternatively activated tumor-associated macrophages are thought to promote angiogenesis and metastasis, in part through paracrine interactions with vascular endothelial cells (28–30) and with tumor cells which promote their invasive potential (20, 31, 32). We therefore asked if *fes-null* macrophages were deficient in these properties. To examine this we cultured primary BMMs from wild-type or *fes-null* mice in isolation or in cocultures with MTLn3 rat mammary adenocarcinoma cells in a collagen matrix-based invasion assay model (20). BMMs from each genotype or MTLn3 cells invaded to the same degree when cultured in isolation. In cocultures, BMMs from both genotypes promoted the invasion of MTLn3 cells, but *fes-null* BMMs were significantly less effective in doing so ($P = 0.005$; Fig. 6). MTLn3 cells also promoted the invasion of BMMs in cocultures, but the *fes-null* BMMs were significantly less responsive ($P = 0.002$; Fig. 6).

Fes-deficiency in the lung niche does not compromise tumor cell invasion and initial growth rates at the metastatic site

Angiogenesis is believed to play a rate-limiting effect on tumor growth. Reduced tumor growth rates at the primary site in *fes-null* mice might therefore be due in part to roles for Fes in promoting vascular endothelial cell migration, proliferation, and establishment of new vessel structures. However, metastasis also involves interactions between tumor and endothelial cells, both at the level of escape from the primary site and extravasation at the metastatic site. To explore this latter event we injected GFP-expressing AC2M2 cells into the tail veins of wild-type and *fes-null nu/nu* mice and quantified the number and sizes of lung metastatic lesions that formed after 22 days using biophotonic imaging of resected lungs (Supplementary Fig. S6). No significant differences were seen, suggesting that Fes-deficiency in the lung microvascular bed did not influence the process of tumor cell adhesion and invasion through the endothelium, or the initial metastatic growth rate.

Downloaded from cancerres.aacrjournals.org on May 16, 2021. © 2011 American Association for Cancer Research.

Published OnlineFirst December 15, 2010; DOI: 10.1158/0008-5472.CAN-10-3757

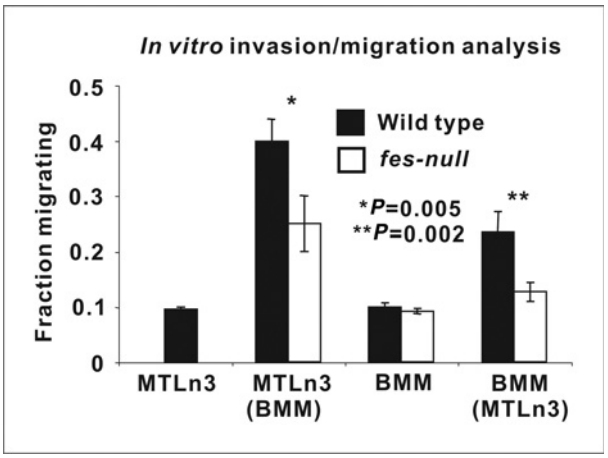

Figure 6. Fes-null macrophages are defective in promoting tumor cell migration and invasion. BMMs were obtained from wild-type and *fes-null* mice and plated in monolayers in isolation or with MTLn3 breast tumor cells. After 16 hours they were overlayed with collagen I gels. Migration/invasion into the collagen after 24 hours was assessed by confocal microscopy and the fraction of each cell type that migrated/invaded 20 μM or more was determined. For the cocultures, the histograms indicate migration of the unbracketed cell type. In cocultures, *fes-null* BMMs were significantly less effective at promoting the migration/invasion of MTLn3 cells than wild-type BMMs ($P = 0.005$). Tumor cell-induced migration/invasion of BMMs was also significantly reduced in *fes-null* relative to wild-type BMMs ($P = 0.002$). The data are the average of 3 independent experiments.

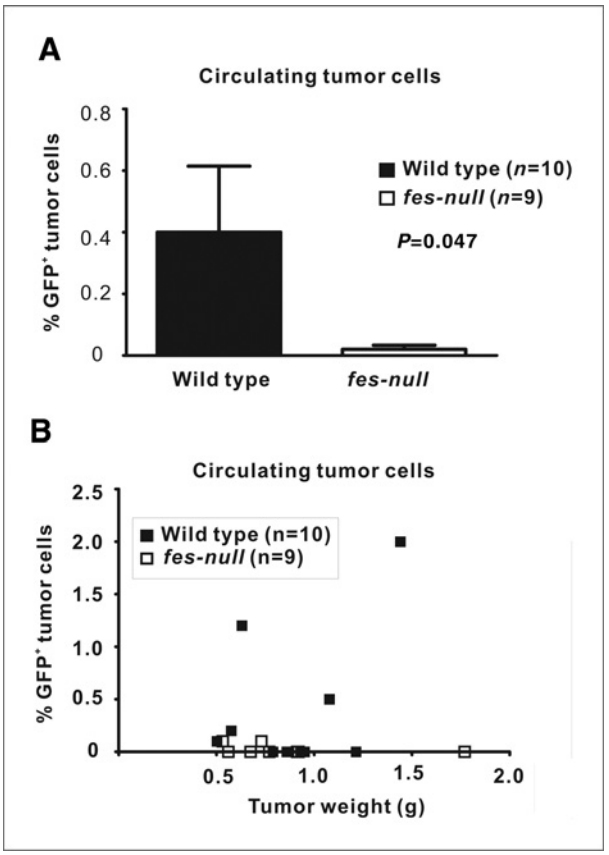

Figure 7. Fes-deficiency in the niche correlated with reduced CTC frequency. Peripheral blood was isolated by cardiac puncture of control mice or tumor-bearing mice 22 days after engraftment with GFP-expressing AC2M2 cells. RBCs were removed by hypotonic lysis and the remaining nucleated cells were assessed for GFP fluorescence by flow cytometry. A, percent GFP^+ nucleated circulating cells ($P = 0.047$, $n = 10$ wild type, $n = 9$ *fes-null*). B, percent GFP^+ cells were plotted against the weight of excised tumors. There were no significant detectable levels of GFP^+ cells in 9 tumor-bearing *fes-null* mice. In contrast, 3 of 10 wild-type tumor-bearing mice had significant levels of GFP^+ cells. Positive and negative controls were nontumor bearing mouse blood with or without spiked addition of GFP-expressing AC2M2 cells.

Fes deficiency in the niche compromises the escape of tumor cells from the primary tumor site

Paracrine signaling between tumor cells and macrophages at the primary tumor site may play an important role in metastasis by promoting the ability of tumor cells to gain access to the vasculature (31–33). Reduced metastasis in *fes-null* mice (Fig. 2) coupled with observations suggesting that Fes may potentiate paracrine signaling between macrophages and tumor cells contributing to mutually enhanced invasive potential (Fig. 6) led us to examine the number of circulating tumor cells (CTC) in this engraftment model. GFP-expressing AC2M2 cells were injected into the mammary glands of wild-type and *fes-null nu/nu* mice and tumors were allowed to grow for 22 days. Peripheral blood was then assessed for the presence of CTCs by flow cytometry (Fig. 7). A significantly higher percentage of GFP^+ nucleated cells was detected in the blood of tumor-bearing wild-type relative to *fes-null* mice ($P = 0.047$; Fig. 7A). Although tumor sizes were smaller in all but one of the *fes-null* mice at the time of analysis, there was no apparent correlation between levels of CTCs and tumor sizes in the wild-type or *fes-null* mice (Fig. 7B).

Discussion

Mammalian Fes and orthologous avian Fps were initially discovered as viral oncogenic PTKs encoded by tumor-causing retroviruses (5, 6). Subsequent studies demonstrated the transforming and tumorigenic potential of those viral Fes/Fps oncoproteins (7). Collectively, those observations argued that cellular Fes, when activated by mutation or inappropriately overexpressed, could promote tumorigenesis through dominant acting tumor cell autonomous functions. We were therefore surprised to find that ectopic overexpression of wild-type, kinase-activated, or kinase-dead cellular Fes had no apparent effect on the *in vivo* tumorigenic potential of the tumor cell line used in these engraftment studies. It should also be noted that we were unable to detect endogenous Fes expression in AC2M2 cells, and Fes does not appear to be expressed in any of the breast cancer cell lines we have examined (data not shown); nor has its expression in breast cancer been reported in the literature, to our knowledge.

Considering that Fes is also expressed in vascular endothelial and myeloid lineages, we next explored the possibility that it might influence tumorigenesis through effects on cells in the tumor niche. We had previously shown that transgenic expression of an activated *fes* allele correlated with hypervascularity, and this led to the original observation of Fes

Downloaded from cancerres.aacrjournals.org on May 16, 2021. © 2011 American Association for Cancer Research.

Published OnlineFirst December 15, 2010; DOI: 10.1158/0008-5472.CAN-10-3757

expression in vascular endothelial cells (11). Subsequent studies have linked Fes activation to signaling in endothelial cells downstream of angiogenic growth factors including VEGF, platelet-derived growth factor (PDGF), and fibroblast growth factor (FGF; refs. 12, 21–23). Using PECAM-1 expression as a marker of endothelial cells, we observed a significant reduction in the vascularity of tumors and associated stroma in *fes-null* mice. There was also a trend toward reduced vascularity in unaffected mammary glands in tumor-bearing mice as well as in glands of control mice; consequently, reduced angiogenesis in *fes-null* mice may not be strictly tumor-associated. However, these latter reductions were not statistically significant, suggesting that tumor-associated angiogenic signaling may be more sensitive to Fes deficiency. Because angiogenesis is linked to tumor growth and metastasis, these observations were consistent with the observed differences in growth rate and lung metastasis. Thus, reduced tumorigenesis in *fes-null* mice may be, at least in part, due to loss of proangiogenic Fes signaling functions intrinsic to vascular endothelial cells, and could reflect differential responsiveness to tumor-produced paracrine acting factors including VEGF, PDGF, and FGF.

Other cells of the niche can interact in a paracrine fashion with the endothelium and with tumor cells to promote tumor growth and metastasis. Fes is also expressed in hematopoietic cell types, including platelets (34), mast cells, (35) granulocytic cell types, (36) and macrophages (16). Although we cannot rule out any particular cell type, we focused our attention on macrophages because of the high level of Fes expression in these cells and accumulating evidence linking them to tumorigenesis (24, 28–30, 33, 37–39). Given our observation of decreased numbers of CTCs in *fes-null* mice, we were particularly intrigued with the recent report correlating tumor cell interactions with macrophages and endothelial cells with clinical metastasis in breast cancer (39). *In vitro* co-culture experiments revealed a significant defect in the ability of *fes-null* bone marrow derived macrophages to promote tumor cell invasion into collagen I gels. Furthermore, the tumor cell-induced invasive properties of the macrophages were compromised in Fes-deficient cells. These observations strongly argue that Fes plays roles in metastasis by promoting paracrine interactions between macrophages and tumor cells. However, it should be considered that BMMs were used in these coculture collagen gel invasion studies, so their precise phenotype may not be expected to precisely recapitulate that of tumor-associated macrophages *in vivo*. Furthermore, the *in vivo* niche contains many other cytokines, growth factors, and extracellular matrix components, as well as many other cell types, including fibroblasts, lymphocytes, and vascular and lymphatic endothelial cells. Further studies are required to elucidate the roles of Fes in differentiation of monocytic progenitors into specialized macrophage phenotypes and the ability of these cells to interact with the *in vivo* tumor niche.

Classically, activated inflammatory M1-like macrophages are induced by IFN-γ as well as other factors including lipopolysaccharide (LPS), TNFα, and granulocyte macrophage colony stimulating factor (GM-CSF); and they mediate resistance to microbial infections as well as antitumorigenic properties (reviewed in ref. 40). Alternatively, activated M2-like macrophages are induced by interleukin (IL)-4 and IL-13; and in response to other cytokines, including TGF-β, IL-10, and CSF-1, they acquire tumor-promoting properties, and also suppress inhibitory M1 macrophage functions (reviewed in ref. 41). We observed fewer phagocytic $F4/80^+$ macrophages in *fes-null* tumor-associated stroma, and we speculate that tumor promoting M2-like macrophages may be reduced in *fes-null* tumor stroma.

Fes-deficient mice had slightly reduced numbers of circulating myeloid cells and slightly increased numbers of GM-CSF induced colony-forming unit granulocyte-macrophage colonies in methylcellulose assays (13, 16). These and other studies have implicated Fes in hematopoietic differentiation along the granulocyte–monocyte lineage. However, there have been no studies that specifically addressed the effects of Fes deficiency on macrophage polarization into M1- versus M2-like phenotypes. However, *in vitro* studies have shown that activated Fes can promote differentiation of bi-potential U937 cells into macrophages at the expense of the alternative granulocytic fate (42) and can also promote survival and granulocytic differentiation of 32D cells upon IL-3 removal (43). These observations indicate subtle roles for Fes in regulating myeloid differentiation that merit further analysis. Perhaps of more relevance to this study, it will be important to determine if Fes modulates the response of monocytes to IFN-γ or IL-4/IL-13, which drive M1- or M2-like polarization, respectively (25, 44). Based on our observations, we speculate that Fes-deficient macrophages will be relatively refractory to IL–4– or IL–13–induced M2-like polarization. Previous studies reported that Fes interacts with the IL-4Rα chain in B cells, and potentiates recruitment of PI3K to IRS2 (45, 46) However, we are unaware of reports linking Fes to IL-4/IL-13 signaling in macrophages. We also speculate that Fes-deficient macrophages will be hypersensitive to M1-polarization. We have previously shown that *fes-null* mice display hyperinflammatory responses to LPS (13), which were further characterized *in vivo* by increased leukocyte recruitment to locally inflamed tissues and increased levels of systemic TNFα (47). Cultured *fes-null* macrophages displayed prolonged LPS-induced activation of NFκB, increased TNFα production, and reduced internalization of the TLR4 receptor complex (14). It will be important to determine if Fes-deficiency promotes an M1-like polarization at the expense of M2 macrophages. In that case, Fes inhibition might not only interfere with tumor-promoting functions of M2 polarized macrophages, but might also promote the M1-based antitumor functions. In our current working model, Fes-deficiency may skew macrophages toward a proinflammatory M1 polarity that could contribute to tumor initiation. This might have played a role in the earlier tumor onset seen in the Fes-deficient MMTV-PymT transgenic mouse model of mammary tumorigenesis (9). At later stages of tumorigenesis where tumor associated macrophages tend to skew more towards a protumorigenic M2 polarized state, Fes-deficiency might attenuate that process, leading to reduced tumor progression, as observed in the orthotopic engraftment model used in this study.

Downloaded from cancerres.aacrjournals.org on May 16, 2021. © 2011 American Association for Cancer Research.

Published OnlineFirst December 15, 2010; DOI: 10.1158/0008-5472.CAN-10-3757

In summary, our observations suggest that systemic inhibition of Fes might provide antitumorigenic benefits in cancer by inhibiting endothelial cell intrinsic angiogenic signaling as well as inhibiting the tumor promoting properties of tumor-associated macrophages.

Disclosure of Potential Conflicts of Interest

No potential conflicts of interest were disclosed.

Acknowledgments

We are grateful to Chris Hall, Jalna Meens, Jeffery Mewburn, and Matthew Gordon for technical assistance.

Grant Support

This research was supported by grants from the Canadian Cancer Society to P.A. Greer (#017338), the National Institutes of Health to E.R. Stanley (RO1 CA25604, PO1 CA 100324, P30 CA13330), and V. Chitu (1K01AR054486), the Canadian Breast Cancer Research Alliance to B.E. Elliott (#14315), and the Terry Fox Foundation-–Canadian Institutes of Health Research Multidisciplinary Training Program in Cancer Research to S. Zhang.

The costs of publication of this article were defrayed in part by the payment of page charges. This article must therefore be hereby marked *advertisement* in accordance with 18 U.S.C. Section 1734 solely to indicate this fact.

Received October 15, 2010; revised November 26, 2010; accepted November 30, 2010; published OnlineFirst February 1, 2011.

References

1. Greer P. Closing in on the biological functions of Fps/Fes and Fer. Nat Rev Mol Cell Biol 2002;3:278–89.
2. Smithgall TE, Rogers JA, Peters KL, Li J, Briggs SD, Lionberger JM, et al. The c-Fes family of protein-tyrosine kinases. Crit Rev Oncog 1998;9:43–62.
3. Haigh J, McVeigh J, Greer P. The fps/fes tyrosine kinase is expressed in myeloid, vascular endothelial, epithelial, and neuronal cells and is localized in the trans-golgi network. Cell Growth Differ 1996;7:931–44.
4. Truesdell PF, Zirngibl RA, Francis S, Sangrar W, Greer PA. fps/fes knockout mice display a lactation defect and the fps/fes tyrosine kinase is a component of E-cadherin-based adherens junctions in breast epithelial cells during lactation. Exp Cell Res 2009;315:2929–40.
5. Shibuya M, Hanafusa T, Hanafusa H, Stephenson JR. Homology exists among the transforming sequences of avian and feline sarcoma viruses. Proc Natl Acad Sci U S A 1980;77:6536–40.
6. Sherr CJ, Fedele LA, Oskarsson M, Maizel J, Woude GV. Molecular cloning of Snyder-Theilen feline leukemia and sarcoma viruses: comparative studies of feline sarcoma virus with its natural helper virus and with Moloney murine sarcoma virus. J Virol 1980;34:200–12.
7. Yee SP, Mock D, Greer P, Maltby V, Rossant J, Bernstein A, et al. Lymphoid and mesenchymal tumors in transgenic mice expressing the v-fps protein-tyrosine kinase. Mol Cell Biol 1989;9:5491–9.
8. Bardelli A, Parsons DW, Silliman N, Ptak J, Szabo S, Saha S, et al. Mutational analysis of the tyrosine kinome in colorectal cancers. Science 2003;300:949.
9. Sangrar W, Zirgnibl RA, Gao Y, Muller WJ, Jia Z, Greer PA. An identity crisis for fps/fes:oncogene or tumor suppressor?Cancer Res 2005;65:3518–22.
10. Shaffer JM, Smithgall TE. Promoter methylation blocks FES protein-tyrosine kinase gene expression in colorectal cancer. Genes Chromosomes Cancer 2009;48:272–84.
11. Greer P, Haigh J, Mbamalu G, Khoo W, Bernstein A, Pawson T. The Fps/Fes protein-tyrosine kinase promotes angiogenesis in transgenic mice. Mol Cell Biol 1994;14:6755–63.
12. Haigh JJ, Ema M, Haigh K, Gertsenstein M, Greer P, Rossant J, et al. Activated Fps/Fes partially rescues the in vivo developmental potential of Flk1-deficient vascular progenitor cells. Blood 2004;103:912–20.
13. Zirngibl RA, Senis Y, Greer PA. Enhanced endotoxin sensitivity in fps/fes-null mice with minimal defects in hematopoietic homeostasis. Mol Cell Biol 2002;22:2472–86.
14. Parsons SA, Greer PA. The Fps/Fes kinase regulates the inflammatory response to endotoxin through down-regulation of TLR4, NF-kappaB activation, and TNF-alpha secretion in macrophages. J Leukoc Biol 2006;80:1522–8.
15. Elliott BE, Tam SP, Dexter D, Chen ZQ. Capacity of adipose tissue to promote growth and metastasis of a murine mammary carcinoma: effect of estrogen and progesterone. Int J Cancer 1992;51:416–24.
16. Senis Y, Zirngibl R, McVeigh J, Haman A, Hoang T, Greer PA. Targeted disruption of the murine fps/fes proto-oncogene reveals that Fps/Fes kinase activity is dispensable for hematopoiesis. Mol Cell Biol 1999;19:7436–46.
17. Ellis C, Moran M, McCormick F, Pawson T. Phosphorylation of GAP and GAP-associated proteins by transforming and mitogenic tyrosine kinases. Nature 1990;343:377–81.
18. Udell CM, Samayawardhena LA, Kawakami Y, Kawakami T, Craig AW. Fer and Fps/Fes participate in a Lyn-dependent pathway from FcepsilonRI to platelet-endothelial cell adhesion molecule 1 to limit mast cell activation. J Biol Chem 2006;281:20949–57.
19. Stanley ER. Murine bone marrow-derived macrophages. Methods Mol Biol 1997;75:301–4.
20. Goswami S, Sahai E, Wyckoff JB, Cammer M, Cox D, Pixley FJ, et al. Macrophages promote the invasion of breast carcinoma cells via a colony-stimulating factor-1/epidermal growth factor paracrine loop. Cancer Res 2005;65:5278–83.
21. Kanda S, Naba A, Miyata Y. Inhibition of endothelial cell chemotaxis toward FGF-2 by gefitinib associates with downregulation of Fes activity. Int J Oncol 2009;35:1305–12.
22. Kanda S, Kanetake H, Miyata Y. Downregulation of Fes inhibits VEGF-A-induced chemotaxis and capillary-like morphogenesis by cultured endothelial cells. J Cell Mol Med 2007;11:495–501.
23. Sangrar W, Mewburn JD, Vincent SG, Fisher JT, Greer PA. Vascular defects in gain-of-function fps/fes transgenic mice correlate with PDGF- and VEGF-induced activation of mutant Fps/Fes kinase in endothelial cells. J Thromb Haemost 2004;2:820–32.
24. Lin EY, Nguyen AV, Russell RG, Pollard JW. Colony-stimulating factor 1 promotes progression of mammary tumors to malignancy. J Exp Med 2001;193:727–40.
25. Mantovani A, Allavena P, Sica A, Balkwill F. Cancer-related inflammation. Nature 2008;454:436–44.
26. Sica A, Bronte V. Altered macrophage differentiation and immune dysfunction in tumor development. J Clin Invest 2007;117:1155–66.
27. Leek RD, Lewis CE, Whitehouse R, Greenall M, Clarke J, Harris AL. Association of macrophage infiltration with angiogenesis and prognosis in invasive breast carcinoma. Cancer Res 1996;56:4625–9.
28. Paulus P, Stanley ER, Schafer R, Abraham D, Aharinejad S. Colony-stimulating factor-1 antibody reverses chemoresistance in human MCF-7 breast cancer xenografts. Cancer Res 2006;66:4349–56.
29. Aharinejad S, Abraham D, Paulus P, Abri H, Hofmann M, Grossschmidt K, et al. Colony-stimulating factor-1 antisense treatment suppresses growth of human tumor xenografts in mice. Cancer Res 2002;62:5317–24.
30. Aharinejad S, Paulus P, Sioud M, Hofmann M, Zins K, Schäfer R, et al. Colony-stimulating factor-1 blockade by antisense oligonucleotides and small interfering RNAs suppresses growth of human mammary tumor xenografts in mice. Cancer Res 2004;64:5378–84.
31. Hernandez L, Smirnova T, Kedrin D, Wyckoff J, Zhu L, Stanley ER, et al. The EGF/CSF-1 paracrine invasion loop can be triggered by heregulin beta1 and CXCL12. Cancer Res 2009;69:3221–7.

Downloaded from cancerres.aacrjournals.org on May 16, 2021. © 2011 American Association for Cancer Research.

Published OnlineFirst December 15, 2010; DOI: 10.1158/0008-5472.CAN-10-3757

32. Wyckoff J, Wang W, Lin EY, Wang Y, Pixley F, Stanley ER, et al. A paracrine loop between tumor cells and macrophages is required for tumor cell migration in mammary tumors. Cancer Res 2004; 64:7022–9.
33. Wyckoff JB, Wang Y, Lin EY, Li JF, Goswami S, Stanley ER, et al. Direct visualization of macrophage-assisted tumor cell intravasation in mammary tumors. Cancer Res 2007;67:2649–56.
34. Senis YA, Sangrar W, Zirngibl RA, Craig AW, Lee DH, Greer PA. Fps/Fes and Fer non-receptor protein-tyrosine kinases regulate collagen- and ADP-induced platelet aggregation. J Thromb Haemost 2003;1:1062–70.
35. Craig AW, Greer PA. Fer kinase is required for sustained p38 kinase activation and maximal chemotaxis of activated mast cells. Mol Cell Biol 2002;22:6363–74.
36. Smithgall TE, Yu G, Glazer RI. Identification of the differentiation-associated p93 tyrosine protein kinase of HL-60 leukemia cells as the product of the human c-fes locus and its expression in myelomonocytic cells. J Biol Chem 1988;263:15050–5.
37. Condeelis J, Pollard JW. Macrophages:obligate partners for tumor cell migration, invasion, and metastasis. Cell 2006;124:263–6.
38. Patsialou A, Wyckoff J, Wang Y, Goswami S, Stanley ER, Condeelis JS. Invasion of human breast cancer cells in vivo requires both paracrine and autocrine loops involving the colony-stimulating factor-1 receptor. Cancer Res 2009;69:9498–506.
39. Robinson BD, Sica GL, Liu YF, Rohan TE, Gertler FB, Condeelis JS, et al. Tumor microenvironment of metastasis in human breast carcinoma: a potential prognostic marker linked to hematogenous dissemination. Clin Cancer Res 2009;15:2433–41.
40. Martinez FO, Gordon S, Locati M, Mantovani A. Transcriptional profiling of the human monocyte-to-macrophage differentiation and polarization:new molecules and patterns of gene expression. J Immunol 2006;177:7303–11.
41. Balkwill F, Charles KA, Mantovani A. Smoldering and polarized inflammation in the initiation and promotion of malignant disease. Cancer Cell 2005;7:211–7.
42. Kim J, Feldman RA. Activated Fes protein tyrosine kinase induces terminal macrophage differentiation of myeloid progenitors (U937 cells) and activation of the transcription factor PU.1. Mol Cell Biol 2002;22:1903–18.
43. Kim J, Ogata Y, Feldman RA. Fes tyrosine kinase promotes survival and terminal granulocyte differentiation of factor-dependent myeloid progenitors (32D) and activates lineage-specific transcription factors. J Biol Chem 2003;278:14978–84.
44. Martinez FO, Helming L, Gordon S. Alternative activation of macrophages: an immunologic functional perspective. Annu Rev Immunol 2009;27:451–83.
45. Izuhara K, Feldman RA, Greer P, Harada N. Interleukin-4 induces association of the c-fes proto-oncogene product with phosphatidylinositol-3 kinase. Blood 1996;88:3910–8.
46. Jiang H, Foltenyi K, Kashiwada M, Donahue L, Vuong B, Hehn B, et al. Fes mediates the IL-4 activation of insulin receptor substrate-2 and cellular proliferation. J Immunol 2001;166:2627–34.
47. Parsons SA, Mewburn JD, Truesdell P, Greer PA. The Fps/Fes kinase regulates leucocyte recruitment and extravasation during inflammation. Immunology 2007;122:542–50.

Downloaded from cancerres.aacrjournals.org on May 16, 2021. © 2011 American Association for Cancer Research.

Published OnlineFirst December 15, 2010; DOI: 10.1158/0008-5472.CAN-10-3757

Cancer Research
The Journal of Cancer Research (1916–1930) | The American Journal of Cancer (1931–1940)

AACR American Association for Cancer Research

Fes Tyrosine Kinase Expression in the Tumor Niche Correlates with Enhanced Tumor Growth, Angiogenesis, Circulating Tumor Cells, Metastasis, and Infiltrating Macrophages

Shengnan Zhang, Violeta Chitu, E. Richard Stanley, et al.

Cancer Res 2011;71:1465-1473. Published OnlineFirst December 15, 2010.

Updated version	Access the most recent version of this article at: doi:10.1158/0008-5472.CAN-10-3757
Supplementary Material	Access the most recent supplemental material at: http://cancerres.aacrjournals.org/content/suppl/2010/12/15/0008-5472.CAN-10-3757.DC1

Cited articles	This article cites 47 articles, 29 of which you can access for free at: http://cancerres.aacrjournals.org/content/71/4/1465.full#ref-list-1
Citing articles	This article has been cited by 3 HighWire-hosted articles. Access the articles at: http://cancerres.aacrjournals.org/content/71/4/1465.full#related-urls

E-mail alerts	Sign up to receive free email-alerts related to this article or journal.
Reprints and Subscriptions	To order reprints of this article or to subscribe to the journal, contact the AACR Publications Department at pubs@aacr.org.
Permissions	To request permission to re-use all or part of this article, use this link http://cancerres.aacrjournals.org/content/71/4/1465. Click on "Request Permissions" which will take you to the Copyright Clearance Center's (CCC) Rightslink site.

Downloaded from cancerres.aacrjournals.org on May 16, 2021. © 2011 American Association for Cancer Research.